

Accelerated induction of *in vitro* apatite formation by parallel alignment of hydrothermally oxidized titanium substrates separated by sub-millimeter gaps

Satoshi Hayakawa, Keigo Okamoto & Tomohiko Yoshioka

To cite this article: Satoshi Hayakawa, Keigo Okamoto & Tomohiko Yoshioka (2019) Accelerated induction of *in vitro* apatite formation by parallel alignment of hydrothermally oxidized titanium substrates separated by sub-millimeter gaps, Journal of Asian Ceramic Societies, 7:1, 90-100, DOI: [10.1080/21870764.2019.1572690](https://doi.org/10.1080/21870764.2019.1572690)

To link to this article: <https://doi.org/10.1080/21870764.2019.1572690>



© 2019 The Author(s). Published by Informa UK Limited, trading as Taylor & Francis Group on behalf of The Korean Ceramic Society and The Ceramic Society of Japan



Accepted author version posted online: 19 Jan 2019.
Published online: 11 Feb 2019.



[Submit your article to this journal](#)



Article views: 322



[View related articles](#)



[View Crossmark data](#)



Citing articles: 2 [View citing articles](#)

Accelerated induction of *in vitro* apatite formation by parallel alignment of hydrothermally oxidized titanium substrates separated by sub-millimeter gaps

Satoshi Hayakawa ^a, Keigo Okamoto^b and Tomohiko Yoshioka^a

^aBiomaterials Laboratory, Graduate School of Interdisciplinary Science and Engineering in Health Systems, Okayama University, Kita-ku, Japan; ^bBiomaterials Laboratory, Graduate School of Natural Science and Technology, Okayama University, Kita-ku, Japan

ABSTRACT

Although autoclaving is a common sterilization method for biomedical devices, the ability to induce deposition of apatite particles on hydrothermally treated titanium is still not fully realized. This is because the induction ability is too weak to be evaluated via *in vitro* apatite formation in Kokubo's simulated body fluid (SBF) by the conventional immersion method, i.e. using samples with open and smooth surface. This study reports on the surface structure of hydrothermally treated titanium and the ability to induce deposition of apatite particles on the surface of parallel confined spaces separated by sub-millimeter gaps in Kokubo's SBF. Thin-film X-ray diffraction and analyses using Fourier transform infra-red (FT-IR) spectroscopy and Raman spectroscopy revealed that a nano-crystalline anatase-type titanium oxide layer was formed on titanium substrates after hydrothermal treatment at 150°C for 2 h. When growth of the titanium oxide layer was moderately suppressed, the hydrothermally treated titanium surface exhibited a characteristic interference color, silver or gold, which does not impair the esthetic appearance of the titanium-based implant. The ability to induce deposition of apatite particles on hydrothermally treated titanium was remarkably amplified by parallel alignment of substrates separated by sub-millimeter gaps.

ARTICLE HISTORY

Received 15 July 2018
Accepted 6 January 2019



KEYWORDS

Titanium substrate; apatite deposition; simulated body fluid; parallel alignment; titania layer

1. Introduction

Since titanium and titanium alloys have excellent mechanical strength, biocompatibility, and corrosion resistance, they are widely used as biomedical implant materials in the orthopedic and dental fields [1,2]. When metallic titanium is embedded in a living body, it is covered with a thin non-collagenous amorphous material [3,4], and thus requires a long period to achieve mechanical fixation, either by bone ingrowth or by interlocking (between bone tissue and the implant). It is therefore necessary to induce spontaneous precipitation of low-crystalline apatite particles on the surface of titanium-based implants in the body to improve bonding with bony tissue. Various surface modification methods have been proposed to improve the osteoconductivity of titanium-based implants [5–10]. We have developed GRAPE® technology [11–15], which spontaneously forms a low-crystalline apatite particle layer on the surfaces of grooves in metallic titanium samples that are soaked in a simulated body fluid (SBF; Kokubo solution [16]) by applying thermal oxidation treatment at 500°C. The induction of apatite formation on the titanium oxide layer was confirmed using sub-millimeter spatial gaps instead of grooves [13–15]. The titanium oxide layer (rutile phase) produced on the titanium

surface due to thermal oxidation did not induce deposition of apatite particles when exposed to bulk SBF [13–15]. The ability of a titanium oxide layer to induce deposition of apatite particles can be amplified by the use of confined spaces. Confining the component ions of apatite or calcium phosphate clusters, such as pre-embryos and embryos, within a narrow space is an essential feature of GRAPE® technology [17]. Since the surface of thermally oxidized implants exhibits a characteristic interference color, such as deep violet due to the titanium oxide layer [18], however, the esthetic appearance (appearance of peri-implant soft tissues) is inferior to the golden or the silver coloring common to dental implants [19]. If the temperature of the thermal oxidation treatment is decreased to reduce the influence of the interference color, the apatite-forming ability decreases remarkably. Depositing a nano-crystalline titanium oxide layer on the titanium surface by chemical and thermal treatment [20–26] or applying anodic oxidation treatment [27–30] can induce the deposition of apatite particles in SBF. Despite this fact, few studies have focused on the esthetic appearance of titanium implants, and the influence of the interference color cannot be avoided due to the deposition of titanium oxide crystallites on the surface. Unfortunately, this

CONTACT Satoshi Hayakawa  satoshi@cc.okayama-u.ac.jp  Biomaterials Laboratory, Graduate School of Interdisciplinary Science and Engineering in Health Systems, Okayama University, Kita-ku, Japan

© 2019 The Author(s). Published by Informa UK Limited, trading as Taylor & Francis Group on behalf of The Korean Ceramic Society and The Ceramic Society of Japan. This is an Open Access article distributed under the terms of the Creative Commons Attribution License (<http://creativecommons.org/licenses/by/4.0/>), which permits unrestricted use, distribution, and reproduction in any medium, provided the original work is properly cited.

means that there must be a trade-off between the ability to deposit apatite particles and the esthetic appearance of titanium implants. Thus far, there are many reports concerning the effects of hydrothermal treatment on the surface of metallic titanium and its physico-chemical and biological properties [31–37]. Fluorine-contaminated titanium implants were strongly discolored after autoclaving (by applying high-pressure steam sterilization treatment at 132°C for 20 min) due to the growth of a surface oxide [38]. The apatite-forming ability of thermally oxidized titanium substrates was enhanced by autoclaving (121°C, 20 min) due to an increase in surface Ti—OH groups [39]. The growth of apatite-like crystals on anodically oxidized titanium was promoted by autoclaving (300°C, 2 h or 4 h) [40]. If a metallic titanium substrate is subjected to hydrothermal treatment, the growth of the titanium oxide layer can be precisely controlled to reduce the influence of the interference color and enable more Ti—OH groups to be formed on the surface than with thermal oxidation. Our preliminary experiments revealed, however, that hydrothermally treated titanium substrates did not induce deposition of apatite particles when exposed to bulk SBF. In this study, hydrothermal treatment was applied to titanium substrates at 150°C for various periods, and the apatite-forming ability of hydrothermally treated titanium substrates separated by sub-millimeter spatial gaps was evaluated after soaking the substrates in SBF for 7 days. We also investigated the surface structure and appearance of the hydrothermally treated titanium substrates and the effects of the storage environment on their apatite-forming ability.

2. Materials and methods

The SBF, prepared according to the formulation proposed by Kokubo et al [16], had an ion concentration similar to that of human blood plasma (Na^+ 142.0, K^+ 5.0, Mg^{2+} 1.5, Ca^{2+} 2.5, Cl^- 147.8, HCO_3^- 4.2, HPO_4^{2-} 1.0, SO_4^{2-} 0.5 mM). The pH was adjusted to 7.4 with TRIS and HCl. A mirror-polished pure titanium sheet

was purchased from Sumitomo Metals Ltd. (Naoetsu, Japan) and rectangular substrates (20 mm × 10 mm × 2 mm) were cut from the sheet. The titanium substrates were ultrasonically washed with acetone for 10 min and then ultrasonically rinsed with ultra-pure water. The hydrothermal treatment can be described as follows: two titanium substrates were placed in a PTFE vessel (50 mL) to which 10 mL of ultra-pure water was then added. The vessel was sealed with a stainless-steel compact pressure vessel and kept in an incubator at 150°C for various periods ranging from 30 min to 24 h. The specimens and configurations are depicted in Figure 1, which shows the two titanium substrates subjected to hydrothermal treatment placed parallel to each other with a gap of 0.3 mm and held together at four corners with an adhesive and polymer (Nylon®) spacers. The titanium specimens were suspended in the center of a tightly capped polyethylene bottle and soaked in 40 mL of SBF (pH7.4, 36.5°C) for up to 7 days. The specimens were then gently rinsed with ultra-pure water and dried in air at room temperature. The surfaces of the hydrothermally treated titanium specimens were examined using a laser Raman spectrometer (JASCO NRS-5100, Japan) with a wavelength of 532 nm and laser power of 11 mW, as well as with a Fourier transform infrared reflection spectrometer (FT-IRRS, Thermo-Fisher Scientific, Nexus 470, USA) equipped with a Model 501 Spectra Tech attachment (reflection angle 75°), which collected the signals from 256 scans at a resolution of 4 cm^{-1} . The spectrum for an as-received mirror-polished titanium substrate was taken as the background. In addition, the surface oxide was examined by an X-ray photoelectron spectrophotometer (XPS, S-Probe ESCA SSX100S, Fisons Instruments, USA) using monochromatized $\text{AlK}\alpha$ radiation ($h\nu = 1486.6$ eV). The binding energy drift was corrected by normalizing the measured binding energy to the $\text{Ti}2\text{p}$ core level of 458.8 eV. The formation of apatite crystals on the surface after being soaked in SBF was examined by using thin-film X-ray diffraction (TFXRD, X'pert-ProMPD, PANalytical, the Netherlands) with $\text{CuK}\alpha$ radiation ($\lambda = 1.5418$ Å) operating at 45 kV and 40 mA, a 2θ scan mode, and an incident angle

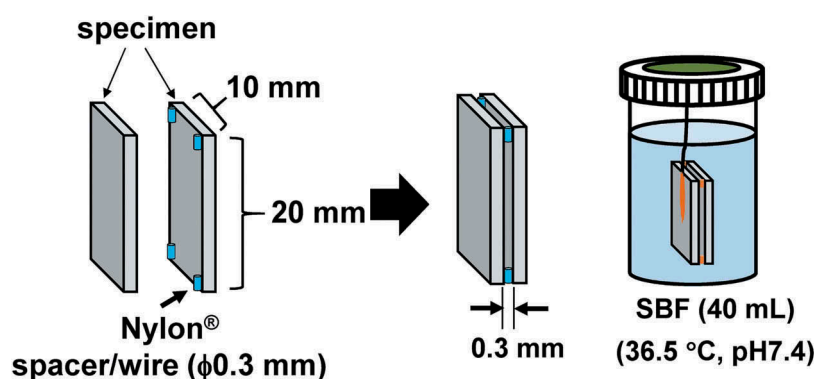


Figure 1. Schematic drawing and configuration of the specimens, in which a pair of titanium specimens is held together at four corners with Nylon® spacers.

θ of 1.0° . The surface morphology was examined by field emission scanning electron microscopy (FE-SEM, S-4800, HITACHI High-Technologies, Japan) with an accelerating voltage of 5 kV and a filament current of 30 μ A. The quantity (number), size, and surface coverage of the deposited apatite particles were derived with image analysis software (Image Pro 4.5, Media Cybernetics, Inc., USA).

3. Results

3.1. Appearance and structure of titanium specimen surface after hydrothermal treatment

The surface of the specimen subjected to hydrothermal treatment for 2 h was lustrous and silver-colored, almost identical to that of mirror-polished titanium substrates (Figure 2). However, the surface color of the specimen subjected to hydrothermal treatment for 24 h was golden. TF-XRD patterns of the titanium specimens before and after hydrothermal treatment are shown in Figure 3. Diffraction peaks belonging to Ti (ICDD PDF#44–1294) were observed at around 2θ angles of 35° and 38° in all the specimens. A peak attributed to anatase (ICDD PDF#21–1272) was identified at 26° (101 diffraction) on the titanium specimens that were hydrothermally treated for 2 and 24 h.

Raman spectra showed characteristic peaks at 394, 513, and 630 cm^{-1} for the specimens subjected to hydrothermal treatment for more than 1 h, which were attributed to Raman bands of the anatase phase, B_{1g} , (A_{1g} , B_{1g}), and E_g , respectively (Figure 4(a)) [41,42]. In addition, FT-IRRS analysis showed reflection peaks at 542 cm^{-1} and 845 cm^{-1} for all the specimens subjected to hydrothermal treatment for more than 1 h, which can be attributed to stretching vibrations of Ti—O—Ti and Ti—O, respectively (Figure 4(b)) [43]. The intensity of the Raman and FT-IRRS peaks corresponding to anatase increased with the hydrothermal treatment time, which was in good agreement with the XRD results.

FE-SEM images of the surfaces of the titanium specimens before and after hydrothermal treatment are shown in Figure 5. It can be seen that nano-scale anatase grains were deposited on the surfaces of all specimens treated for 1 h or more. Formation of

densely packed anatase grains can be observed on the surfaces of specimens treated for 24 h, indicating that the numerical density of grains increased with increases in the hydrothermal treatment time.

Figure 6 shows O1s core spectra obtained by XPS measurement for the specimens subjected to hydrothermal treatment for 1 h and 2 h. The spectra can be deconvoluted into a few peaks, according to Healy et al. [44,45]. The largest peak at 530.1 eV is derived from the oxygen atoms located in the crystal lattice of titanium oxide. The peak at 532.1 eV is derived from the OH group, in which a proton is coordinated with the oxygen atom on the titanium oxide surface, also called a bridging oxygen (Ti—O—Ti), and water molecules physically adsorbed on the titanium oxide surface. The peak at 534.2 eV is derived from the oxygen atoms in terminal Ti—OH. The hydroxyl group chemically adsorbed to the titanium atom on the titanium oxide surface. The latter two peaks are referred to as acidic Ti—OH groups and basic Ti—OH groups, respectively [46]. It can be suggested that both acidic and basic Ti—OH groups are formed on the surface of titanium specimens subjected to hydrothermal treatment. The fraction of the peaks corresponding to acidic and basic Ti—OH groups revealed that the amount of acidic and basic Ti—OH groups increased with increases in the hydrothermal treatment time. It can therefore be concluded that a nano-crystalline anatase-type titanium oxide layer possessing acidic and basic Ti—OH groups is formed on the surface of metallic titanium substrates after hydrothermal treatment.

3.2. In vitro apatite-forming ability of hydrothermally treated titanium specimens

The results of naked-eye inspection of the titanium specimens showed that the apatite formation was induced on the contact surface but not on the open surface. Figure 7 shows TF-XRD patterns of contact surfaces of titanium specimens hydrothermally treated for various periods, and then soaked in SBF for 7 days. Peaks attributed to HAp (ICDD PDF#09–0432) were detected at 2θ angles of 26° (HAp 002 diffraction) and 32° (HAp 211 and 112 diffractions) in the XRD patterns of the titanium specimens hydrothermally

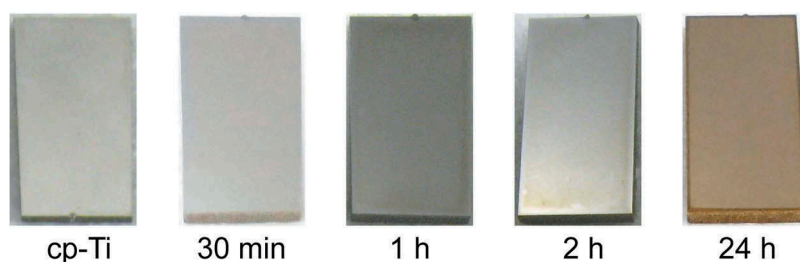


Figure 2. Photo images of the surfaces of titanium specimens before and after hydrothermal treatment for 30 min, 1 h, 2 h, and 24 h.

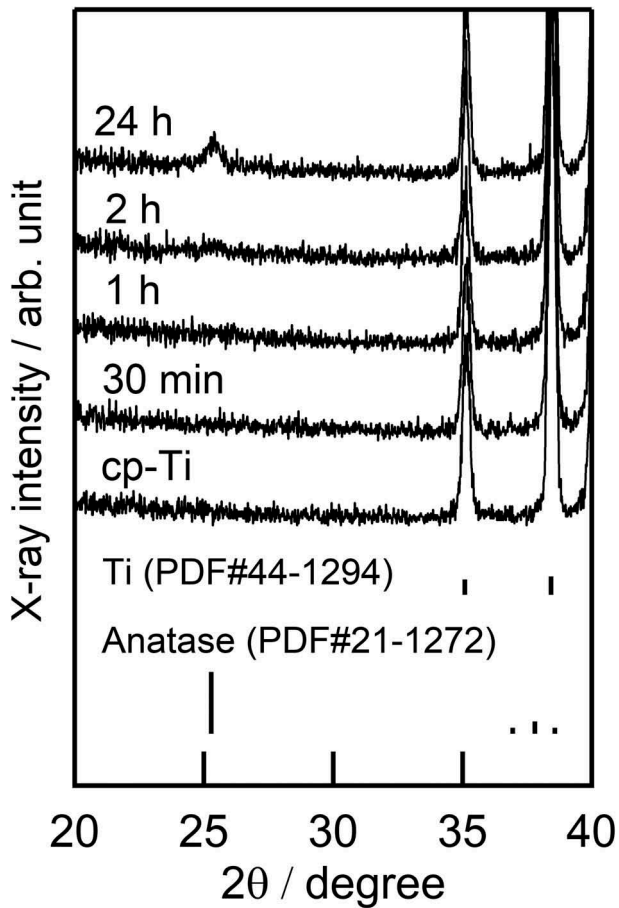


Figure 3. TF-XRD patterns of titanium specimens before and after hydrothermal treatment for 30 min, 1 h, 2 h, and 24 h.

treated for more than 2 h. Figure 8 shows TF-XRD patterns of the surfaces of titanium specimens hydrothermally treated for 2 h and soaked in SBF for various

periods up to 7 days. Diffraction peaks corresponding to HAp appeared after 1 day, and the area of the diffraction peak at 32° increased with longer immersion periods (Figure 9). Figure 10 shows FE-SEM images of the central regions of the contact surfaces of these titanium specimens. Very few nano-apatite crystallites were observed on the specimen surfaces after soaking in SBF for 6 h. Nano-apatite crystallites, present as small hemispherical particles, appeared on the specimen surfaces after soaking in SBF for 1 day. In order to evaluate the degree of deposition of apatite particles on the specimens, the quantity (number), size, and surface coverage of the particles calculated from FE-SEM images are summarized in Figure 11. The number and size of the hemispherical particles increased with immersion periods of up to 3 days, whereas the surface coverage gradually increased with immersion periods of up to 5 days, which is consistent with the changes in the peak area of HAp diffraction as shown in Figure 9. The results indicated that apatite particles could be deposited on the surface of hydrothermally treated titanium specimens after soaking in SBF for a period as short as 1 day under parallel conditions of alignment with a sub-millimeter gap between specimens.

3.3. Effect of the storage environment of hydrothermally treated titanium substrates on their apatite-forming ability

Titanium substrates subjected to hydrothermal treatment for 2 h were stored under conditions of either sealed air or polar media (water or acetone) for up to

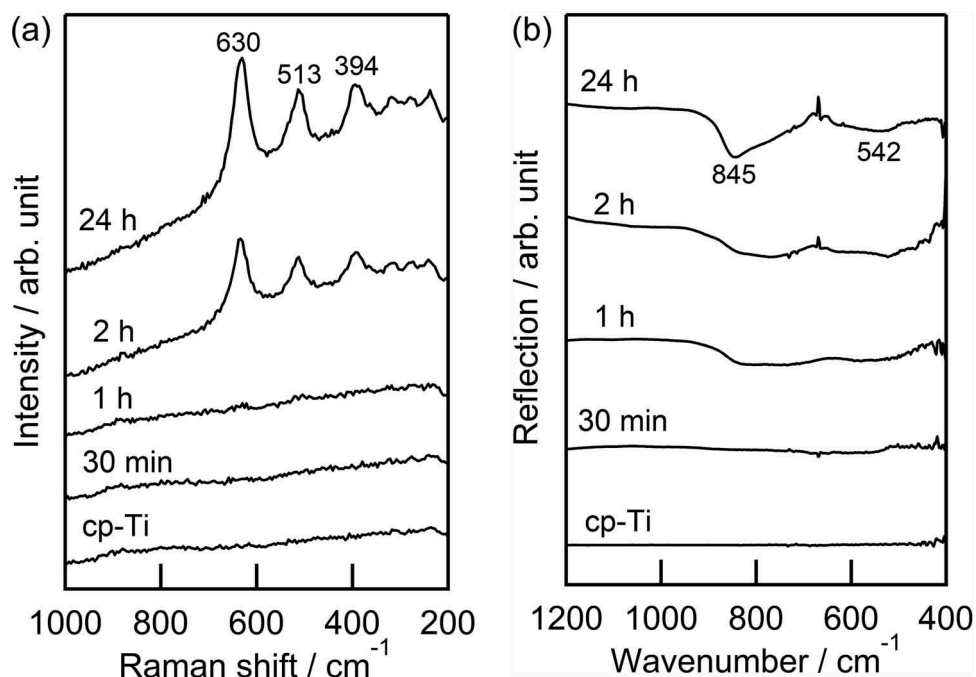


Figure 4. (a) Raman spectra of titanium specimens before and after hydrothermal treatment for 30 min, 1 h, 2 h, and 24 h. (b) FT-IRRS spectra of titanium specimens before and after hydrothermal treatment for 30 min, 1 h, 2 h, and 24 h.

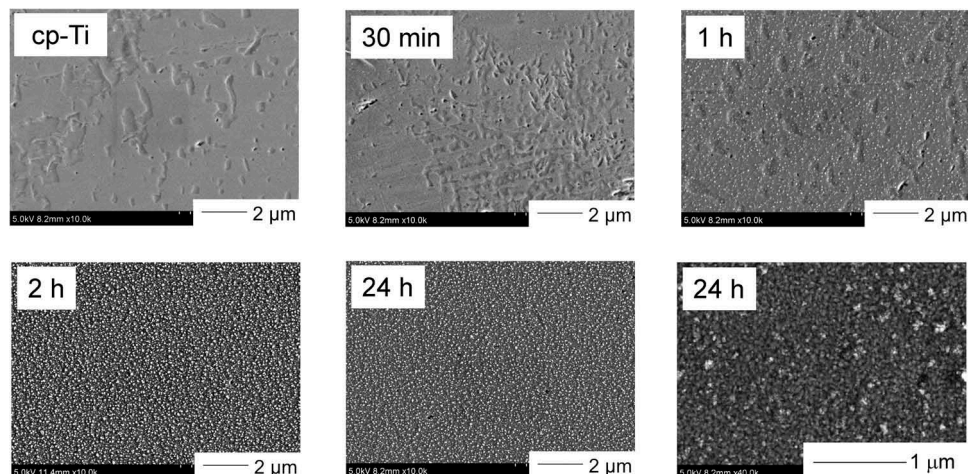


Figure 5. FE-SEM images of titanium specimens before and after hydrothermal treatment for 30 min, 1 h, 2 h, and 24 h.

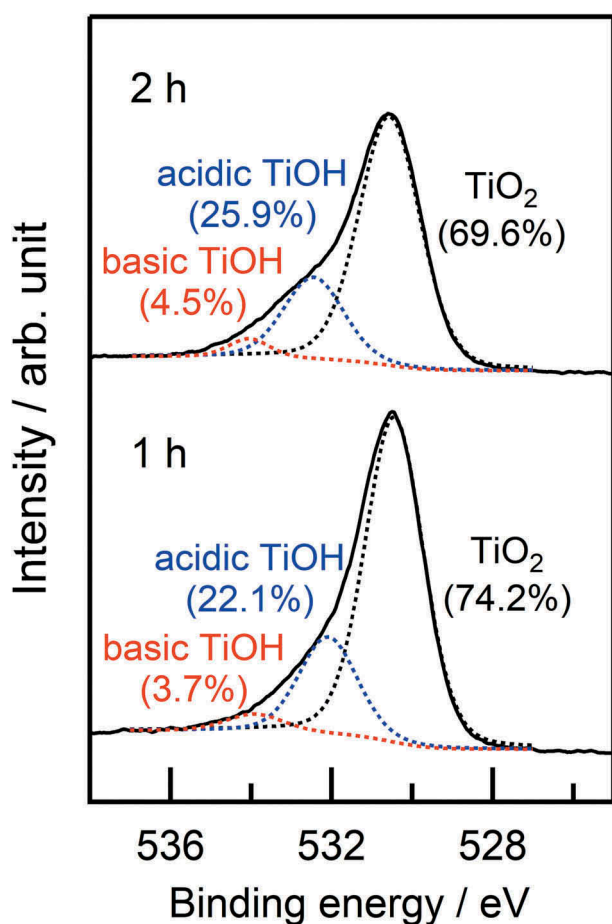


Figure 6. O1s XPS spectra of titanium specimens after hydrothermal treatment for 1 h and 2 h.

6 months in a dark place at room temperature. For storage in sealed air, the titanium substrate was placed in a polystyrene case with a cover. For a storage in water, the specimen was first placed in a 40-mL polystyrene bottle. Then ultra-pure water equivalent to about half of the bottle volume (20 mL) was added, and the bottle was tightly capped. For storage in acetone, the substrate was placed in a screw-capped bottle, into which acetone equivalent to about half of the

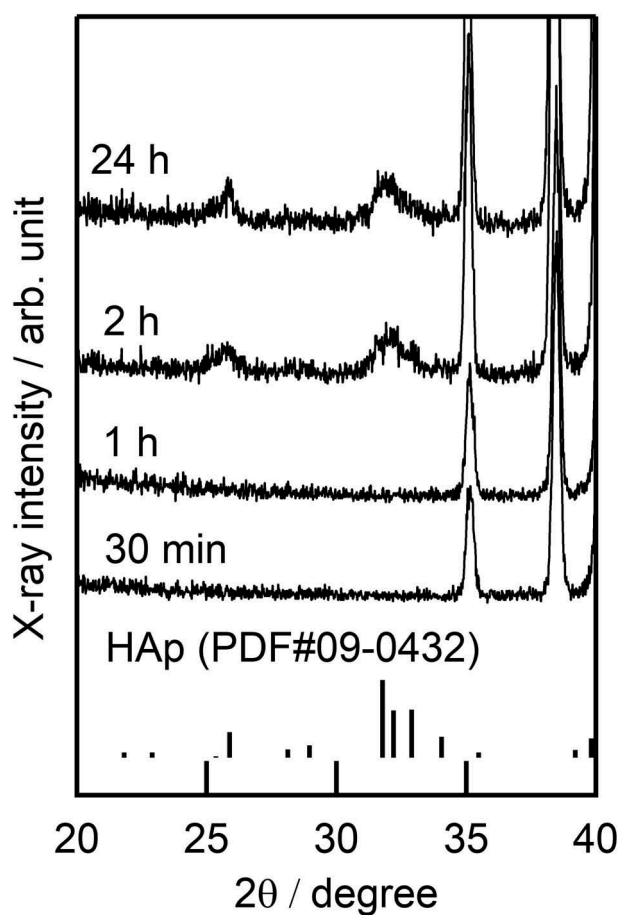


Figure 7. TF-XRD patterns of the contact surfaces of hydrothermally treated titanium specimens after soaking in SBF at 36.5°C for 7 days.

bottle volume was added, and the bottle was tightly capped. After the storage period, two titanium substrates were aligned with a parallel gap of 0.3 mm as shown in Figure 1. The titanium specimens were suspended in the center of a tightly capped polyethylene bottle and soaked in 40 mL of SBF (pH7.4, 36.5°C) for 7 days. Figure 12 shows TF-XRD patterns of the contact surfaces of titanium specimens stored in various

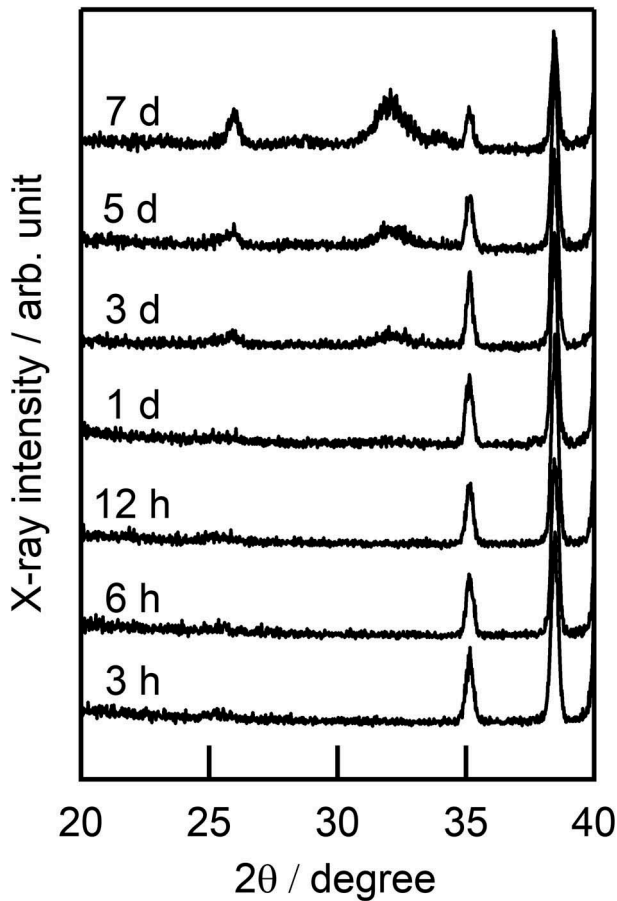


Figure 8. TF-XRD patterns of the contact surfaces of hydrothermally treated titanium specimens (2 h) after soaking in SBF at 36.5°C for various periods from 3 h to 7 days.

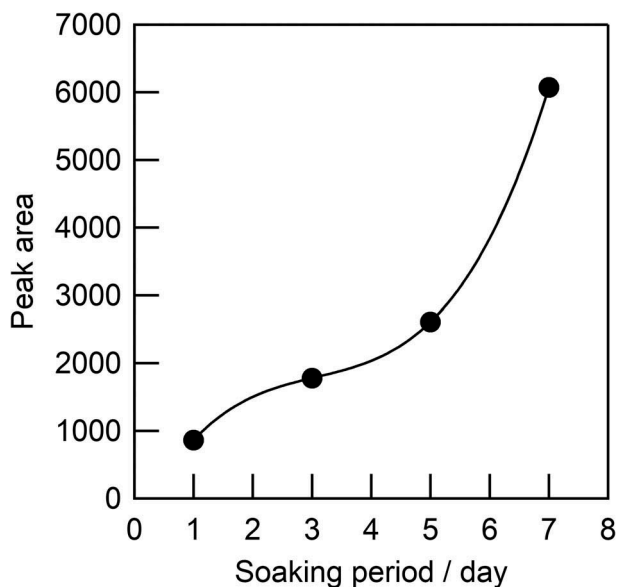


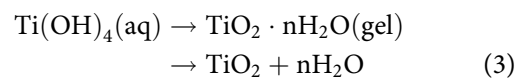
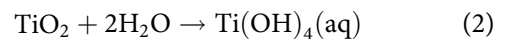
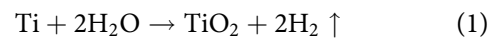
Figure 9. Diffraction peak area of the 32°-apatite peak as a function of soaking period.

environments after soaking in SBF for 7 days. Peaks belonging to HAp (ICDD PDF#09-0432) were detected at around 2θ angles of 26° and 32° for all the specimens except the one stored in sealed air for 2 months. Figure 13 shows that the 32° peak area

remained unchanged for all the storage periods. This indicates that the apatite-forming ability of hydrothermally oxidized titanium specimens is not affected by storage conditions for up to 6 months.

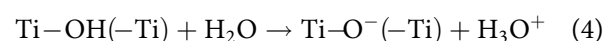
4. Discussion

The reaction mechanism of hydrothermal treatment of pure Ti has been elucidated by several researchers [33–36]. According to the model suggested by Hamada et al. [34] and Shi et al. [36], when pure Ti is subjected to hydrothermal treatment, the chemical reactions can be described as follows:



It can be expected, therefore, that hydrothermal conditions promote oxidation of pure Ti and deposition of TiO_2 in water (Eq. (1)), which then induces subsequent growth of anatase-type titanium oxide crystals via dissolution (Eq. (2)) and precipitation (Eq. (3)), depending on the reaction temperature and time. It can therefore be suggested that anatase-type titanium oxide nano-crystals are grown on the surface of titanium substrates by hydrothermal oxidation of metallic titanium substrates in water.

Deposition of apatite particles was induced on the contact surface of hydrothermally treated titanium specimens in SBF within 1 day when they were aligned with a parallel gap of 0.3 mm. We found that the commencement of the deposition of apatite particles on the surface requires at least 2 h of hydrothermal treatment. Previous studies have reported that heterogeneous nucleation of apatite may be induced by Ti—OH groups, either on the hydrated titanium oxide layer [23–25,47] or through the epitaxial effects of the specific arrangement of the groups on the exposed crystal facet [24,48,49]. Recently, Xiao et al. reported that {101} facets of rutile contributed to inducing deposition of apatite particles [50]. The O1s core XPS spectra of hydrothermally treated titanium specimens (Figure 6) were deconvoluted into three peaks at 530.1, 532.1, and 534.2 eV, which can be assigned to the oxygen atoms in the crystal lattice of titanium oxide, the oxygen atoms of acidic Ti—OH(—Ti) groups or adsorbed water molecules, and the oxygen atoms of basic Ti—OH groups on the surface, respectively. An acidic Ti—OH(—Ti) groups works as a proton-donor and a negatively charged site, while a basic Ti—OH group works as a proton-acceptor or a positively charged site in SBF (pH7.4), as illustrated by the following equations:



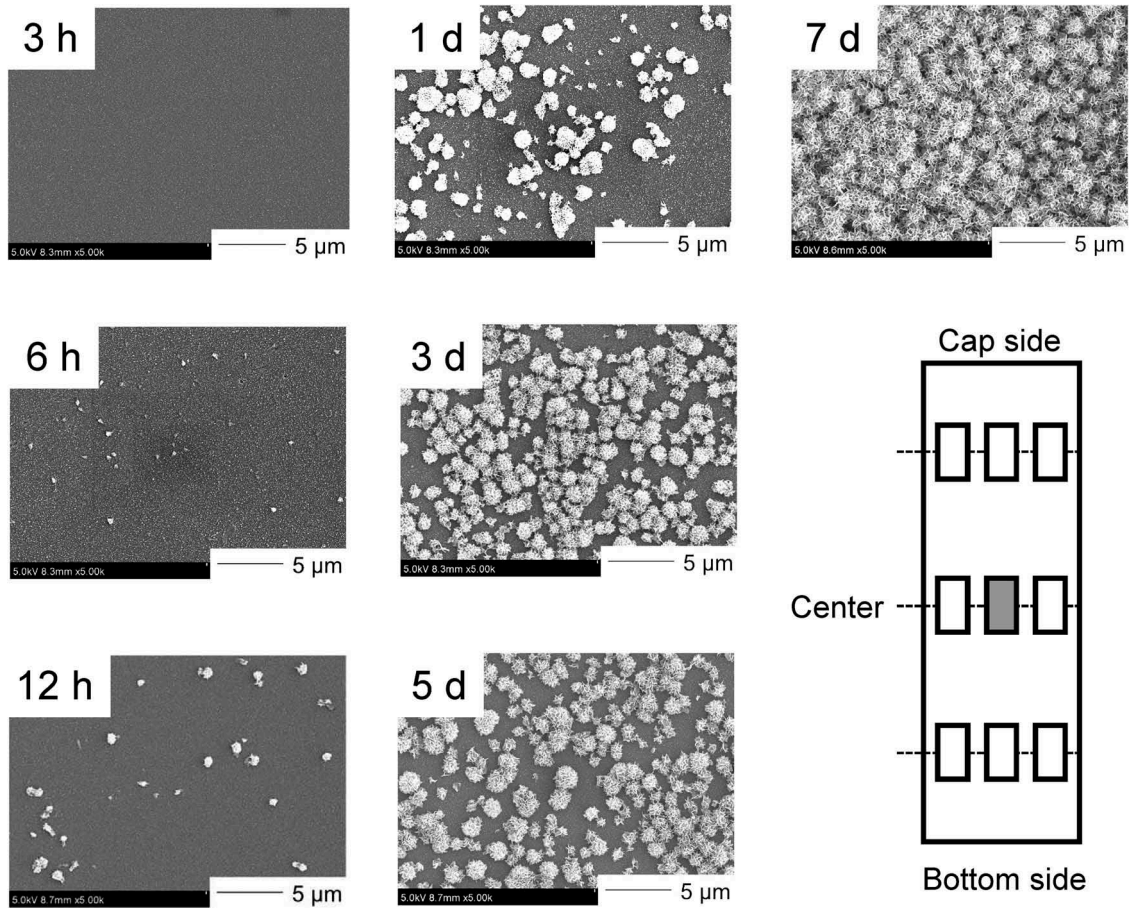


Figure 10. FE-SEM images of the central region of the contact surfaces of hydrothermally treated titanium specimens (2 h) aligned parallel to each other and soaked in a SBF at 36.5°C for various periods from 3 h to 7 days.

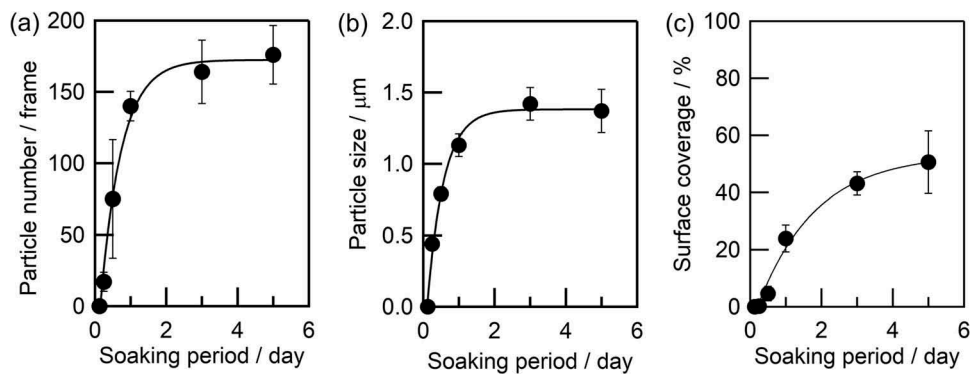
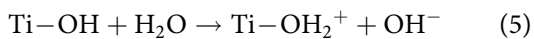


Figure 11. (a) Number, (b) size, and (c) surface coverage of hemispherical particles as a function of the soaking period in SBF. Results were evaluated for the central region of the contact surfaces of hydrothermally treated titanium specimens (2 h) with a spatial gap of 0.3-mm.



According to the model proposed by Uetsuki et al. [51], the hydrated titanium oxide layer contains adequate assemblies of acidic Ti—OH(—Ti) and basic Ti—OH groups to which the component ions and species of apatite can be attached. Indeed, deposition of apatite particles was discerned on sol-gel derived titanium oxide after soaking in SBF for 1–2 weeks [47,52–54]. In addition, previous studies reported that a nano-crystalline titanium oxide layer had

apatite particles deposited on the surface after soaking in SBF for 1–2 days [25,49,51]. The induction periods for apatite nucleation on the titanium oxide layer should be dependent on both the numerical density of the Ti—OH groups and adequate assemblies of acidic Ti—OH(—Ti) and basic Ti—OH groups. In our case, however, a nano-crystalline anatase-type titanium oxide layer on hydrothermally treated titanium substrates did not induce deposition of apatite particles when the surface was exposed to bulk SBF. The significant difference between the

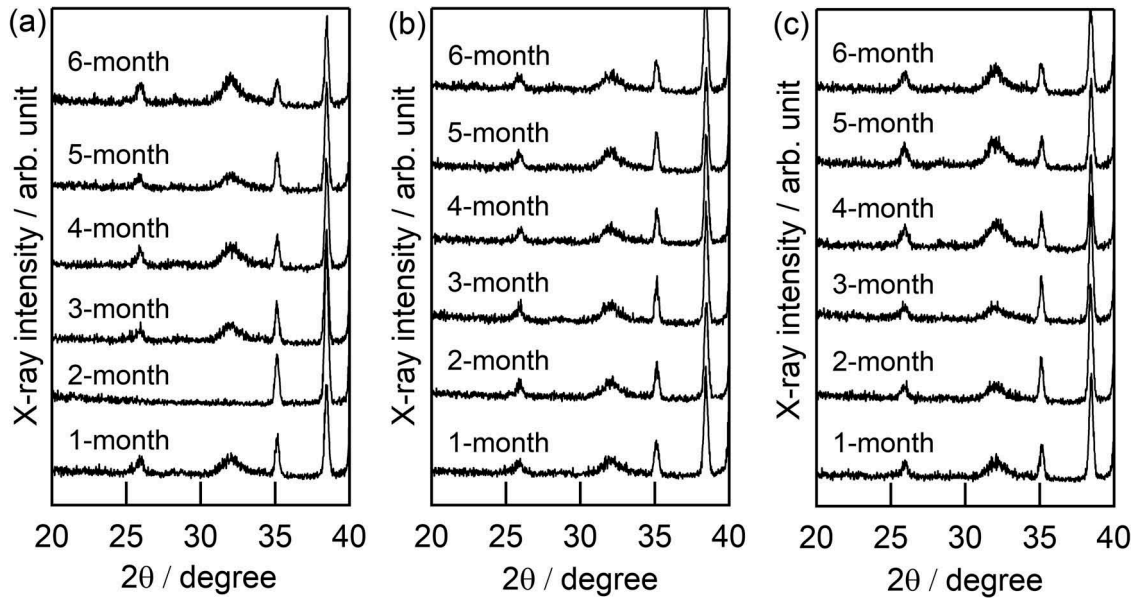


Figure 12. TF-XRD patterns of the contact surfaces of hydrothermally treated titanium specimens (2 h) after soaking in SBF at 36.5°C for 7 days. The titanium specimens were stored in (a) air, (b) water, and (c) acetone for various periods from 1 month to 6 months.

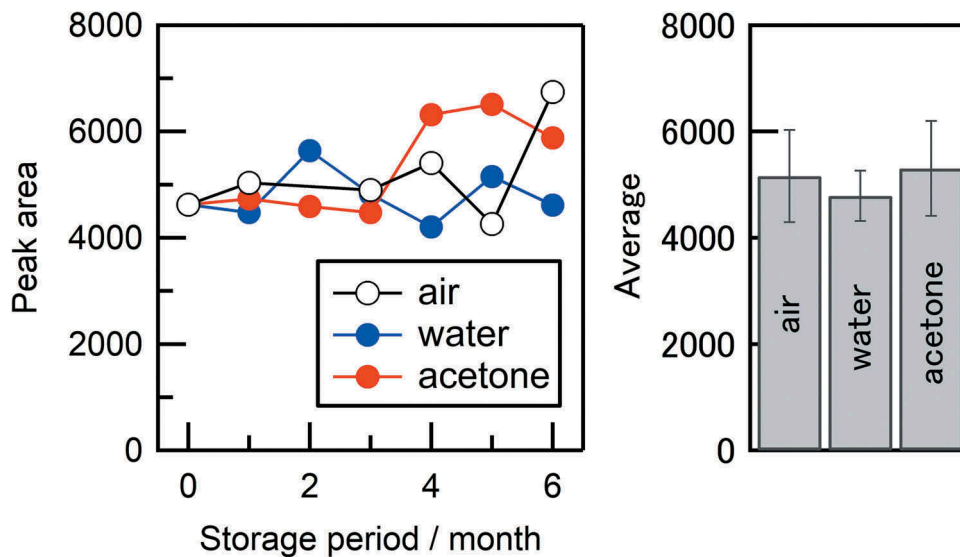


Figure 13. Diffraction peak area of the 32°-apatite peak as a function of storage period in air, water, and acetone. The average values are also shown for purpose of comparison.

hydrothermally prepared titanium oxide layer in this study and the titanium oxide layer prepared by other processing methods is the numerical density of the Ti—OH groups. It can be assumed that the numerical density of the Ti—OH groups in the hydrothermally treated titanium specimen was too small to induce deposition of apatite particles in SBF without a confined space. On the other hand, parallel alignment separated by a sub-millimeter gap remarkably amplified the ability of hydrothermally treated titanium specimens to induce *in vitro* deposition of apatite particles within 1 day. Our previous study reported that the component ions and species of apatite diffusing in a confined space contributed to

nucleation and growth of apatite crystallites on active sites, i.e. acidic Ti—OH(—Ti) and basic Ti—OH groups [17]. Hence, the rate of nucleation and growth of apatite particles on the active sites can be accelerated by introducing a narrow sub-millimeter gap between parallel-aligned titanium specimens. According to the model proposed by Uetsuki et al. [51], hemispherical apatite particles can be formed via primary heterogeneous nucleation and growth of apatite on the hydrated titanium oxide layer, followed by secondary nucleation, growth and aggregation. The total number of hemispherical apatite particles corresponds to the number of active sites involved in the primary nucleation process, while the size of the

hemispherical apatite particles depends on the nucleation induction time. The size of the hemispherical apatite particles formed on the hydrothermally treated titanium substrates in this study (1.4 μm in diameter) is in fair agreement with that reported by Nakao et al. [39]. If we assume that the hemispherical apatite particles have a constant diameter and are closely packed on a flat surface, the ideal estimated coverage are ca. 78% and the density of active sites for apatite nucleation and growth can be calculated from the following equation [55]:

$$\begin{aligned} \text{Active - site density (site count/m}^2\text{)} \\ = (\sqrt{3}r^2)^{-1} \end{aligned} \quad (6)$$

where r is the hemispherical particle diameter. The calculated active-site density for the hydrothermally oxidized titanium specimen is $2.95 \times 10^{11} \text{ m}^{-2}$, 4 times higher than that of the thermally oxidized titanium specimen, $6.86 \times 10^{10} \text{ m}^{-2}$. We can conclude therefore that hydrothermally oxidized titanium specimens exhibited a higher active site density than thermally oxidized titanium substrates. The striking difference in the calculated values can be explained by the fact that the rate of the nucleation is controlled not only by active-site density, but also by the environment in which the active sites are present. If we assume that a finite number of active sites, with low activity for apatite nucleation, are widely distributed on the hydrated titanium oxide surface, parallel alignment with a sub-millimeter gap limits the diffusion of the component ions and apatite species near these active sites. This enhances the interaction between the active sites and the component ions and apatite species, resulting in accelerated nucleation and growth. Consequently, the present results provide important insights into the effect of confined spaces on amplification of the apatite-forming ability of materials. This study also corroborates the use of hydrothermal oxidation in the fabrication process of titanium-based implants in various types of confined space, such as grooves, cavities, gaps, pores, and tubes. From the viewpoints of an evaluation method for the *in vitro* apatite-forming ability of materials, confined spaces are more suitable than open surfaces. A confined space can be used as a facile method for searching for materials with low apatite-forming ability using a conventional SBF solution instead of various concentrated SBF solutions.

5. Conclusion

Titanium substrates were hydrothermally oxidized at 150°C for various periods, from 30 min up to 24 h. The formation of a nano-crystalline anatase-type titanium oxide layer on the surfaces of titanium substrates was confirmed after hydrothermal treatment for at least 2 h. Hydrothermally treated titanium substrates aligned

parallel to each other and separated by a sub-millimeter gap in SBF induced the deposition of apatite particles on the contact surfaces within 1 day. These findings suggest that the accelerated induction of deposition of apatite particles can be ascribed to the synergy effects of active-site density on the titanium oxide surface and the confined space resulting from the sub-millimeter gap.

Acknowledgments

We would also like to thank Editage (www.editage.jp) for English language editing.

Disclosure statement

No potential conflict of interest was reported by the authors.

Funding

This study was supported by JSPS KAKENHI Grant Number 24656386. The authors would like to thank Mr. Hiroomi Kimura and Dr. Keita Uetsuki of Teijin-Nakashima Medical Co., Ltd. for their assistance with the Raman measurement and SEM observation.

ORCID

Satoshi Hayakawa  <http://orcid.org/0000-0002-1097-8614>

References

- [1] Geetha M, Singh AK, Asokamani R, et al. Ti based biomaterials, the ultimate choice for orthopaedic implant – A review. *Prog Mater Sci.* 2009;54(3):397–425.
- [2] Ratner BD. A perspective on Titanium Biocompatibility. In: Brunette DM, Tengvall P, Textor M, et al., editors. *Titanium in medicine: materials science, surface science, engineering, biological responses and medical applications.* Vol. I, Berlin: Springer; 2001. p. 1–12.
- [3] Albrektsson T, Brånemark PI, Hansson HA, et al. The interface zone of inorganic implants *In vivo*: titanium implants in bone. *Ann Biomed Eng.* 1983;11(1):1–27.
- [4] Thomsen P, Larsson C, Ericson LE, et al. Structure of the interface between rabbit cortical bone and implants of gold, zirconium and titanium. *J Mater Sci Mater Med.* 1997;8(11):653–665.
- [5] Liu X, Chu PK, Ding C. Surface modification of titanium, titanium alloys, and related materials for biomedical applications. *Mater Sci Eng R.* 2004;47(3–4):49–121.
- [6] Duan K, Wang R. Surface chemistry of bone implant through wet chemistry. *J Mater Chem.* 2006;16(24):2309–2321.
- [7] Liu X, Chu PK, Ding C. Surface nano-functionalization of biomaterials. *Mater Sci Eng R.* 2010;70(3–6):275–302.
- [8] Minagar S, Berndt CC, Wang J, et al. A review of the application of anodization for the fabrication of nanotubes on metal implant surfaces. *Acta Biomater.* 2012;8(8):2875–2888.

- [9] Salou L, Hoornaert A, Louarn G, et al. Enhanced osseointegration of titanium implants with nanostructured surfaces: an experimental study in rabbits. *Acta Biomater.* 2015;11(1):494–502.
- [10] Camargo WA, Takemoto S, Hoekstra JW, et al. Effect of surface alkali-based treatment of titanium implants on ability to promote *in vitro* mineralization and *in vivo* bone formation. *Acta Biomater.* 2017;57(15):511–523.
- [11] Wang X-X, Hayakawa S, Tsuru K, et al. A comparative study of *in vitro* apatite deposition on heat-, H₂O₂-, and NaOH-treated titanium surfaces. *J Biomed Mater Res.* 2001;54(2):172–178.
- [12] Wang -X-X, Yan W, Hayakawa S, et al. Apatite deposition on thermally and anodically oxidized titanium surfaces in simulated body fluid. *Biomaterials.* 2003;24(25):4631–4637.
- [13] Sugino A, Ohtsuki C, Tsuru K, et al. Effect of spatial design and thermal oxidation on apatite formation on Ti-15Zr-4Ta-4Nb alloy. *Acta Biomater.* 2009;5(1):298–304.
- [14] Sugino A, Tsuru K, Hayakawa S, et al. Induced deposition of bone-like hydroxyapatite on thermally oxidized titanium substrates using a spatial gap in a solution that mimics a body fluid. *J Ceram Soc Japan.* 2009;117(4):515–520.
- [15] Sugino A, Uetsuki K, Kuramoto K. GRAPE technology or bone-like apatite deposition in narrow grooves. In: Narayan R, Colombo P, Mathur S et al., editors. *Advances in bioceramics and porous ceramics III, ceramic engineering and science proceedings*. Vol. 31, Columbus: The American Ceramic Society; 2010. p. 57–62.
- [16] Kokubo T, Takadama H. How useful is SBF in predicting *in vivo* bone bioactivity? *Biomaterials.* 2006;27(15):2907–2915.
- [17] Hayakawa S, Tsuru K, Uetsuki K, et al. Calcium phosphate crystallization on titania in a flowing Kokubo solution. *J Mater Sci Mater Med.* 2015;26(8):222.
- [18] Gaul E. Coloring titanium and related metals by electrochemical oxidation. *J Chem Educ.* 1993;70(3):176–178.
- [19] Ishikawa-Nagai S, Da Silva JD, Weber HP, et al. Optical phenomenon of peri-implant soft tissue. Part II. preferred implant neck color to improve soft tissue esthetics. *Clin Oral Implants Res.* 2007;18(5):575–580.
- [20] Kokubo T, Miyaji F, Kim H-M, et al. Spontaneous formation of bone-like apatite layer on chemically treated titanium metals. *J Am Ceram Soc.* 1996;79(4):1127–1129.
- [21] Kim H-M, Miyaji F, Kokubo T, et al. Preparation of bioactive Ti and its alloy via simple chemical surface treatment. *J Biomed Mater Res.* 1996;32(3):409–417.
- [22] Wen HB, De Wijn JR, Cui FZ, et al. Preparation of bioactive Ti6Al4V surfaces by a simple method. *Biomaterials.* 1998;19(1–3):215–221.
- [23] Ohtsuki C, Iida H, Hayakawa S, et al. Bioactivity of titanium treated with hydrogen peroxide solution containing metal chlorides. *J Biomed Mater Res.* 1997;35(1):39–47.
- [24] Wang X-X, Hayakawa S, Tsuru K, et al. Improvement of the bioactivity of H₂O₂/TaCl₅-treated titanium after a subsequent heat treatment. *J Biomed Mater Res.* 2000;52(1):171–176.
- [25] Wang X-X, Hayakawa S, Tsuru K, et al. Bioactive titania gel layers formed by chemical treatment of Ti substrate with a H₂O₂/HCl solution. *Biomaterials.* 2002;23(5):1353–1357.
- [26] MacDonald DE, Rapuano BE, Deo N, et al. Thermal and chemical modification of titanium-aluminum-vanadium implant materials: effects on surface properties, glycoprotein adsorption, and MG63 cell attachment. *Biomaterials.* 2004;25(16):3135–3146.
- [27] Yang B, Uchida M, Kim H-M, et al. Preparation of bioactive titanium metal via anodic oxidation treatment. *Biomaterials.* 2004;24(6):1003–1010.
- [28] Frauchiger VM, Schlottig F, Gasser B, et al. Anodic plasma-chemical treatment of CP titanium surfaces for biomedical application. *Biomaterials.* 2004;25(4):593–606.
- [29] Cui X, Kim H-M, Kawashita M, et al. Preparation of bioactive titania films on titanium metal via anodic oxidation. *Dent Mater.* 2009;25(1):80–86.
- [30] Kulkarni M, Mazare A, Gongadze E, et al. Titanium nanostructures for biomedical applications. *Nanotechnology.* 2015;26(6):062002.
- [31] Keller JC, Draughn RA, Wightman JP, et al. Characterization of sterilized CP titanium implant surfaces. *Int J Oral Maxillofac Implant.* 1990;5(4):50–67.
- [32] De Andrade MC, Sader MS, Filgueiras MRT, et al. Microstructure of ceramic coating on titanium surface as a result of hydrothermal treatment. *J Mater Sci Mater Med.* 2000;11(11):751–755.
- [33] Cheng FT, Shi P, Man HC. A preliminary study of TiO₂ deposition on NiTi by a hydrothermal method. *Surf Coat Technol.* 2004;187(1):26–32.
- [34] Hamada K, Kon M, Hanawa T, et al. Hydrothermal modification of titanium surface in calcium solutions. *Biomaterials.* 2002;23(10):2265–2272.
- [35] Zhang L, Ayukawa Y, LeGeros RZ, et al. Tissue-response to calcium-bonded titanium surface. *J Biomed Mater Res.* 2010;95A(1):33–39.
- [36] Shi X, Nakagawa M, Kawachi G, et al. Surface modification of titanium by hydrothermal treatment in Mg-containing solution and early osteoblast responses. *J Mater Sci Mater Med.* 2012;23(5):1281–1290.
- [37] Oshiro W, Ayukawa Y, Atsuta I, et al. Effects of CaCl₂ hydrothermal treatment of titanium implant surfaces on early epithelial sealing. *Colloids Surf B-Biointerfaces.* 2015;131(1):141–147.
- [38] Lausmaa J, Kasemo B, Hansson S. Accelerated oxide growth on titanium implants during autoclaving caused by fluorine contamination. *Biomaterials.* 1985;6(1):23–27.
- [39] Nakao Y, Sugino A, Tsuru K, et al. Enhancement of apatite-forming ability of parallel aligned Ti-substrates with optimum gaps by autoclaving. *J Ceram Soc Japan.* 2010;118(6):483–486.
- [40] Rodriguez R, Kim K, Ong JL. *In vitro* osteoblast response to anodized titanium and anodized titanium followed by hydrothermal treatment. *J Biomed Mater Res.* 2004;65A(3):352–358.
- [41] Balachandran U, Eror NG. Raman spectra of titanium dioxide. *J Solid State Chem.* 1982;42(3):276–282.
- [42] Robert TD, Laude LD, Geskin VM, et al. Micro-Raman spectroscopy study of surface transformations induced by excimer laser irradiation of TiO₂. *Thin Solid Films.* 2003;440(1–2):268–277.
- [43] Urlaub R, Posset U, Thull R. FT-IR spectroscopic investigations on sol-gel-derived coatings from acid-modified titanium alkoxides. *J Non-Cryst Solid.* 2000;265(3):276–284.

- [44] Healy KE, Ducheyne P. The mechanism of passive dissolution of titanium in a model physiological environment. *J Biomed Mater Res.* **1992**;26(3):319–338.
- [45] Healy KE, Ducheyne P. Hydration and preferential molecular adsorption on titanium. *Biomaterials.* **1992**;13(8):553–561.
- [46] Böhm HP. Acidic and basic properties of hydroxylated metal oxide surfaces. *Discuss Faraday Soc.* **1971**;52:264–275.
- [47] Li P-J, Ohtsuki C, Kokubo T, et al. The role of hydrated silica, titania, and alumina in inducing apatite on implants. *J Biomed Mater Res.* **1994**;28(1):7–15.
- [48] Uchida M, Kim H-M, Kokubo T, et al. Structural dependence of apatite formation on titania gels in a simulated body fluid. *J Biomed Mater Res.* **2003**;64A(1):164–170.
- [49] Wu J-M, Hayakawa S, Tsuru K, et al. Low-temperature preparation of anatase and rutile layers on titanium substrates and their ability to induce in vitro apatite deposition. *J Am Ceram Soc.* **2004**;87(9):1635–1642.
- [50] Xiao F, Jiang G-Q, Chen J-Y, et al. Apatite-forming ability of hydrothermally deposited rutile nano-structural arrays with exposed {101} facets on Ti foil. *J Mater Sci.* **2018**;53(1):285–294.
- [51] Uetsuki K, Nakai S, Shirosaki Y, et al. Nucleation and growth of apatite on an anatase layer irradiated with UV light under different environmental conditions. *J Biomed Mater Res Part A.* **2013**;101A(3):712–719.
- [52] Shozui T, Tsuru K, Hayakawa S, et al. Characterization of sol-gel derived titania films on titanium and biomimetic apatite-formation. *Key Eng Mater.* **2006**;309–311:717–720.
- [53] Shozui T, Tsuru K, Hayakawa S, et al. In vitro apatite-forming ability of titania films depends on their substrates. *Key Eng Mater.* **2007**;330–332:633–636.
- [54] Shozui T, Tsuru K, Hayakawa S, et al. XPS study on potential suppression factors of suppressing in vitro apatite formation on anatase films prepared on various substrates. *Surf Coat Technol.* **2009**;203(16):2181–2185.
- [55] Hayakawa S, Masuda Y, Okamoto K, et al. Liquid phase deposited titania coating to enable in vitro apatite formation on Ti6Al4V alloy. *J Mater Sci Mater Med.* **2014**;25(2):375–381.